Suche nach Elektroweakinos mit dem ATLAS Detektor

Ludwig-Maximilians-Universität München
Fakultät für Physik

Dissertation

Eric Schanet

March 2021

Supervisor: PD Dr. Jeanette Lorenz

Notes

Part I

Fundamental concepts

Part II

The 1-lepton analysis

Chapter 8

Results

This chapter discusses the results of the different fit configurations and hypothesis tests performed in the analysis. After the background estimation obtained through a background-only fit in the control regions (CRs) is validated in the validation regions (VRs), the signal regions (SRs) are unblinded and the observed data is compared to the Standard Model of Particle Physics (SM) background expectation.

8.1 Background-only fit results

8.1.1 Results in the control regions

As all CRs are mutually exclusive, a background-only fit simultaneously using information from all CRs can be run. Only the terms for the CRs enter the likelihood as channels and any signal contamination present in the CRs is neglected. This allows to fit the dominant backgrounds to data, and thus by construction leads to a good agreement between observed data and the total fitted background estimate in all CRs. The free normalisation parameters for $t\bar{t}$ (μ_{T}), single top (μ_{ST}) and $W + \text{jets}$ (μ_{W}) are fitted to be

$$\begin{aligned} \mu_{\mathrm{T}} &= 1.02^{+0.07}_{-0.09}, \\ \mu_{\mathrm{ST}} &= 0.6^{+0.5}_{-0.25}, \\ \mu_{\mathrm{W}} &= 1.22^{+0.26}_{-0.24}. \end{aligned} \tag{8.1}$$

While the dominant $t\bar{t}$ background stays roughly at its nominal expectation with respect to MC simulation, $W + \text{jets}$ processes are scaled up. The single top expectation, on the other hand, is scaled down. The high uncertainty on μ_{ST} can be attributed to the relatively low MC statistics as well as the comparably low purity of single top events in STR.

Table 8.1 summarises the fitted background estimate including all uncertainties for all control regions. As discussed in chapter 6, $t\bar{t}$ is the most dominant in all control regions except WR where $W + \text{jets}$ is the largest background, followed by single top and $W + \text{jets}$ processes. Small contributions come from diboson, multiboson as well as other backgrounds like $t\bar{t}+V$, $t\bar{t}+h$ and $V + h$. All processes estimated directly from MC simulation cumulatively account for only 10%,

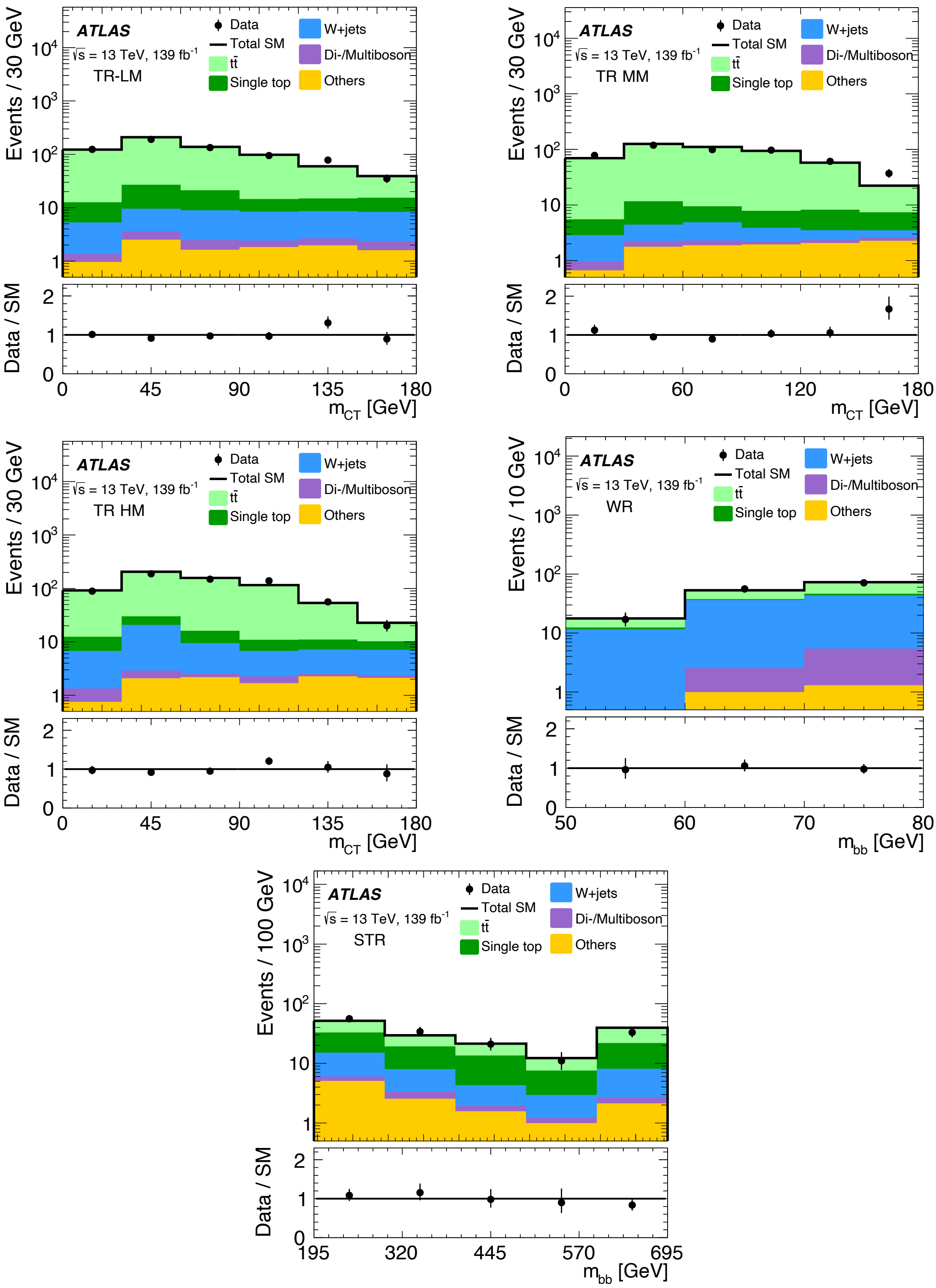

Figure 8.1: Exemplary distribution shown in each control region after the background-only fit. The shaded region includes all systematic uncertainties as well as Monte Carlo (MC) statistical uncertainty. The $t\bar{t}$, single top and $W+$jets are normalised simultaneously in all CRs. A good agreement between MC expectation and data is observed in all CRs.

Table 8.1: Background-only fit results for the CRs for an integrated luminosity of $139\,\text{fb}^{-1}$. Nominal MC expectations (normalised to MC cross-sections) are given for comparison. The errors shown include the MC statistical and systematic uncertainties. PDG rounding is applied to the event rates and uncertainties.

Region	TRLM	TRMM	TRHM	WR	STCR
Observed events	657	491	641	144	155
Fitted SM events	666 ± 25	480 ± 21	645 ± 26	143 ± 12	154 ± 15
$t\bar{t}$	560 ± 40	430 ± 33	550 ± 40	47 ± 9	59 ± 12
Single top	60 ± 40	27 ± 23	33 ± 27	5 ± 4	57 ± 22
$W +$jets	34 ± 8	10.5 ± 2.8	44 ± 11	83 ± 16	23 ± 6
Di-/Multiboson	4.3 ± 1.2	2.0 ± 0.5	2.8 ± 0.5	5.7 ± 1.0	2.8 ± 0.9
Other	10.5 ± 1.3	10.6 ± 1.4	11.1 ± 1.4	2.4 ± 0.4	12.3 ± 1.5
MC exp. SM events	720 ± 80	474 ± 33	680 ± 50	130 ± 13	180 ± 50
$t\bar{t}$	570 ± 70	407 ± 30	570 ± 40	46 ± 10	52 ± 10
Single top	102 ± 18	46 ± 13	58 ± 16	9 ± 6	90 ± 40
$W +$jets	29 ± 4	8.4 ± 1.2	36.1 ± 3.1	67 ± 5	19.0 ± 2.0
Di-/Multiboson	4.1 ± 1.1	2.0 ± 0.5	2.8 ± 0.5	5.6 ± 1.0	2.8 ± 0.9
Other	10.6 ± 1.3	10.6 ± 1.4	11.2 ± 1.4	2.5 ± 0.4	12.4 ± 1.5

5.5% and a maximum of 2.6% in the single top, $W +$jets and $t\bar{t}$ control regions, respectively. Exemplary distributions in the CRs after the background-only fit are shown in fig. 8.1, revealing a good agreement between observed data and the SM background estimate throughout the distributions shown.

8.1.2 Results in the validation regions

In order to validate the extrapolations from the CRs to the SRs, the results of the background-only fit in are extrapolated into the VRs. Table 8.2 details the observed data and background estimation before and after the fit in the different VR bins.

In the on-peak VRs, $t\bar{t}$ is by far the dominant background. Contributions from single top and $W +$jets each amount to only 1–5%, depending on validation region bin. Diboson, multiboson and other SM processes result in minor contributions of the level of not more than 3% of the total background estimate. As the total uncertainties on the background estimate in the on-peak regions are dominated by the $t\bar{t}$ uncertainties, the large uncertainties on the $W +$jets and single top estimate due to relatively limited MC statistics do not have a significant impact. In the off-peak VRs, $t\bar{t}$ is the dominant process in the low mass regime, while contribution from single top and $W +$jets are subdominant. In the medium and high mass regimes, $t\bar{t}$, single top and $W +$jets all result in similar contributions. Diboson, multiboson and other SM processes are only minor backgrounds in all off-peak regions, cumulatively amounting to only 10–14% of the total background estimate depending on the mass regime. Exemplary N-1 distributions in the validation regions after the results from the background-only fit are shown in fig. 8.2.

The agreement between data and the background estimate is summarised in **??**. The background estimates agree within 1.5σ with the observed data in all validation regions, except for the VR-

quote exact numbers

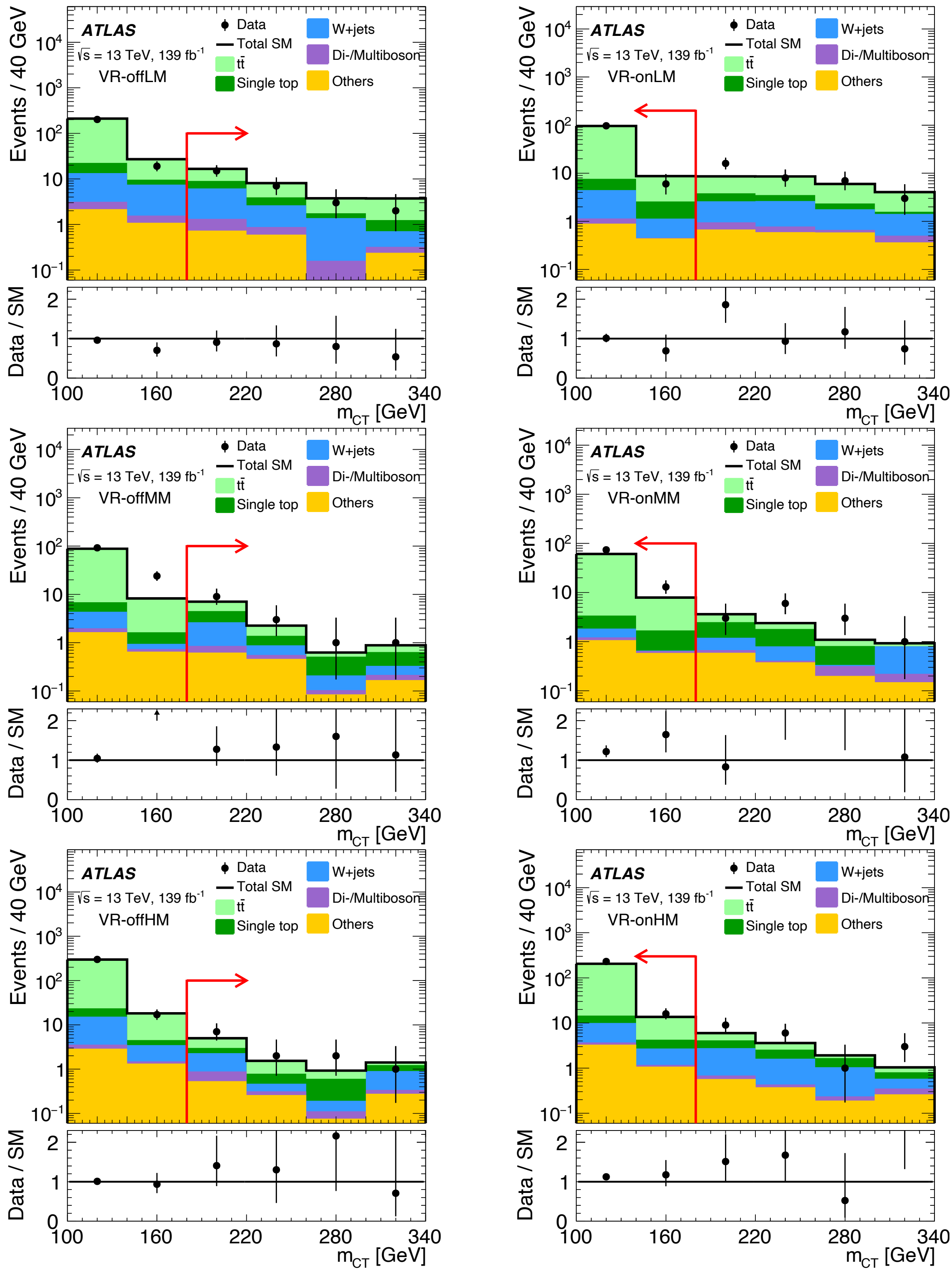

Figure 8.2: Exemplary distributions shown in each validation region after the background-only fit with subsequent extrapolation to the VRs. All selection cuts except for the requirement on m_{CT} (indicated using the red arrow) are applied. The shaded region includes all systematic uncertainties as well as MC statistical uncertainty.

Table 8.2: Background-only fit results from the CRs extrapolated to the VRs for an integrated luminosity of 139 fb^{-1}. Nominal MC expectations (normalised to MC cross-sections) are given for comparison. The errors shown include the MC statistical and systematic uncertainties. Uncertainties in the fitted yields are symmetric by construction, except where the negative error is truncated at an event rate of zero. PDG rounding is applied to the event rates and uncertainties.

Region	VR-onLM	VR-onMM	VR-onHM	VR-offLM	VR-offMM	VR-offHM
Observed events	103	87	247	27	14	12
Fitted SM events	100 ± 19	64 ± 9	215 ± 18	34 ± 6	9.5 ± 2.7	7.5 ± 2.6
$t\bar{t}$	90 ± 19	59 ± 9	196 ± 19	18 ± 4	2.4 ± 1.4	1.8 ± 1.8
Single top	5^{+5}_{-5}	$2.6^{+2.9}_{-2.6}$	6 ± 6	5 ± 4	3.0 ± 1.8	1.8 ± 1.5
$W +$ jets	4 ± 4	0.6 ± 0.5	7.9 ± 2.1	8.2 ± 2.6	2.3 ± 0.8	2.2 ± 0.6
Di-/Multiboson	0.24 ± 0.08	0.19 ± 0.08	0.54 ± 0.19	1.07 ± 0.27	0.39 ± 0.11	0.51 ± 0.14
Other	1.34 ± 0.22	1.67 ± 0.28	4.4 ± 2.0	1.6 ± 0.5	1.34 ± 0.25	1.15 ± 0.24
MC exp. SM events	110 ± 40	69 ± 17	218 ± 22	34 ± 7	12.8 ± 3.4	9.7 ± 3.3
$t\bar{t}$	92 ± 35	62 ± 17	196 ± 21	16 ± 5	3.8 ± 2.2	3.1 ± 1.9
Single top	8 ± 5	4.5 ± 3.4	11 ± 6	9 ± 4	5.3 ± 2.2	3.1 ± 2.5
$W +$ jets	2.8 ± 2.3	0.5 ± 0.5	6.5 ± 1.2	6.5 ± 1.6	2.0 ± 0.5	1.80 ± 0.34
Di-/Multiboson	0.24 ± 0.07	0.19 ± 0.08	0.50 ± 0.17	1.07 ± 0.28	0.37 ± 0.10	0.50 ± 0.15
Other	1.35 ± 0.23	1.70 ± 0.28	4.4 ± 0.9	1.6 ± 0.5	1.36 ± 0.25	1.16 ± 0.24

onMM where the agreement is within 1.9σ. Thus, the overall agreement in the validation regions is considered to be acceptable, paving the way for further extrapolation of the background estimate into the SRs.

8.1.3 Results in the signal regions

By extrapolating the results from the background-only fit in the control regions, the background estimate in the signal regions can be obtained. Table 8.3 compares the background estimate with the observed data for all discovery signal regions. In the low mass discovery signal region, $t\bar{t}$ is the dominant background, followed by $W +$ jets and single top. In the medium mass discovery signal region, all three main backgrounds contribute at roughly equal parts. In the high mass signal region, $W +$ jets is the largest SM background, followed by single top and $t\bar{t}$. In all discovery signal regions, diboson, multiboson and other SM backgrounds yield only minor contributions. The results in the exclusion signal regions are shown in table 8.4. As for the discovery signal regions, $t\bar{t}$ is the dominant background in the low mass signal region bins, while $W +$ jets slightly dominates in the high mass signal region bins. The m_{CT} distribution in all three exclusion SRs are shown in **??**.

None of the exclusion or discovery signal regions reveal a significant deviation from the SM background estimate in data, meaning that all observations are compatible with the SM. Consequently, the signal regions will be used in the following to derive model-dependent as well as model-independent limits. A slight overfluctuation of data in the discovery SRs (that are not mutually exclusive) is quantified to be within 2σ, resulting in weaker model-independent limits than expected. Some of the exclusion signal region bins also exhibit slight overfluctuations in

Table 8.3: Background-only fit results extrapolated to the discovery SRs for an integrated luminosity of 139 fb^{-1}. Nominal MC expectations (normalised to MC cross-sections) are given for comparison. The errors shown include the MC statistical and systematic uncertainties. Uncertainties in the fitted yields are symmetric by construction, except where the negative error is truncated at an event yield of zero. PDG rounding is applied to the event rates and uncertainties.

Region	SR-LM (disc.)	SR-MM (disc.)	SR-HM (disc.)
Observed events	66	32	14
Fitted SM events	47 ± 6	21 ± 5	8.6 ± 2.8
Fitted ttbar events	22 ± 4	5.9 ± 1.9	1.9 ± 0.7
Fitted singletop events	9 ± 6	6 ± 5	$2.0^{+2.4}_{-2.0}$
Fitted wjets events	11.1 ± 2.9	5.6 ± 1.4	3.7 ± 1.0
Fitted diboson events	1.23 ± 0.24	0.56 ± 0.11	0.21 ± 0.06
Fitted Z+jets events	4.8 ± 0.5	2.6 ± 0.4	0.74 ± 0.16
MC exp. SM events	50 ± 7	22 ± 5	8 ± 4
MC exp. ttbar events	21 ± 5	4.9 ± 1.6	1.2 ± 0.6
MC exp. singletop events	14 ± 4	9 ± 5	$2.9^{+3.5}_{-2.9}$
MC exp. wjets events	9.1 ± 1.3	4.5 ± 0.7	3.0 ± 0.6
MC exp. diboson events	1.20 ± 0.23	0.56 ± 0.11	0.21 ± 0.06
MC exp. Z+jets events	4.8 ± 0.5	2.6 ± 0.4	0.74 ± 0.16

data, all well within 2σ of the SM background estimate. Thus, the observed model-dependent exclusion limit derived in section 8.2 is slightly weaker than expected. Figure 8.4 summarises for all regions the observed data, SM background estimate as well as the significances of any deviations.

Table 8.4: Background-only fit results in the exclusion SRs for an integrated luminosity of 139 fb^{-1}. The first column shows the sum of all m_{CT} bins (including overflow). Subsequent columns indicate the different bins in m_{CT}, overflow is included in the last bin. The errors shown include the MC statistical and systematic uncertainties. Uncertainties in the fitted yields are symmetric by construction, except where the negative error is truncated at an event yield of zero. PDG rounding is applied to the event rates and uncertainties.

SR-LM	All m_{CT} bins	Low m_{CT}	Medium m_{CT}	High m_{CT}
Observed	34	16	11	7
Expected	27 ± 4	8.8 ± 2.8	11.3 ± 3.1	7.3 ± 1.5
$t\bar{t}$	16.2 ± 3.4	4.4 ± 2.2	7.3 ± 2.5	4.6 ± 1.2
Single top	2.7 ± 1.8	1.3 ± 1.1	$0.9^{+1.0}_{-0.9}$	0.6 ± 0.6
W+jets	5.5 ± 2.0	2.0 ± 0.9	2.4 ± 1.3	1.1 ± 0.5
Di-/Multiboson	0.67 ± 0.19	0.39 ± 0.13	$0.09^{+0.11}_{-0.09}$	0.18 ± 0.04
Others	2.23 ± 0.29	0.81 ± 0.25	0.64 ± 0.15	0.77 ± 0.12
SR-MM	All m_{CT} bins	Low m_{CT}	Medium m_{CT}	High m_{CT}
Observed	13	4	7	2
Expected	8.6 ± 2.2	4.6 ± 1.7	2.6 ± 1.3	1.4 ± 0.6
$t\bar{t}$	2.7 ± 1.4	1.6 ± 0.9	0.8 ± 0.7	0.30 ± 0.24
Single top	2.7 ± 1.9	1.6 ± 1.5	$1.0^{+1.1}_{-1.0}$	$0.15^{+0.19}_{-0.15}$
W+jets	1.5 ± 0.7	0.6 ± 0.4	$0.3^{+0.4}_{-0.3}$	0.57 ± 0.26
Di-/Multiboson	0.29 ± 0.08	0.09 ± 0.04	0.065 ± 0.028	0.14 ± 0.06
Others	1.33 ± 0.27	0.69 ± 0.20	0.40 ± 0.13	0.24 ± 0.09
SR-HM	All m_{CT} bins	Low m_{CT}	Medium m_{CT}	High m_{CT}
Observed	14	6	5	3
Expected	8.1 ± 2.7	4.1 ± 1.9	2.9 ± 1.3	1.1 ± 0.5
$t\bar{t}$	1.4 ± 0.5	0.8 ± 0.4	0.36 ± 0.25	0.22 ± 0.15
Single top	$2.0^{+2.4}_{-2.0}$	$0.9^{+1.5}_{-0.9}$	0.9 ± 0.9	$0.16^{+0.26}_{-0.16}$
W+jets	3.7 ± 1.0	1.9 ± 0.8	1.4 ± 0.8	0.45 ± 0.19
Di-/Multiboson	0.21 ± 0.06	0.057 ± 0.025	0.075 ± 0.027	0.08 ± 0.04
Others	0.74 ± 0.16	0.34 ± 0.09	0.19 ± 0.08	0.21 ± 0.08

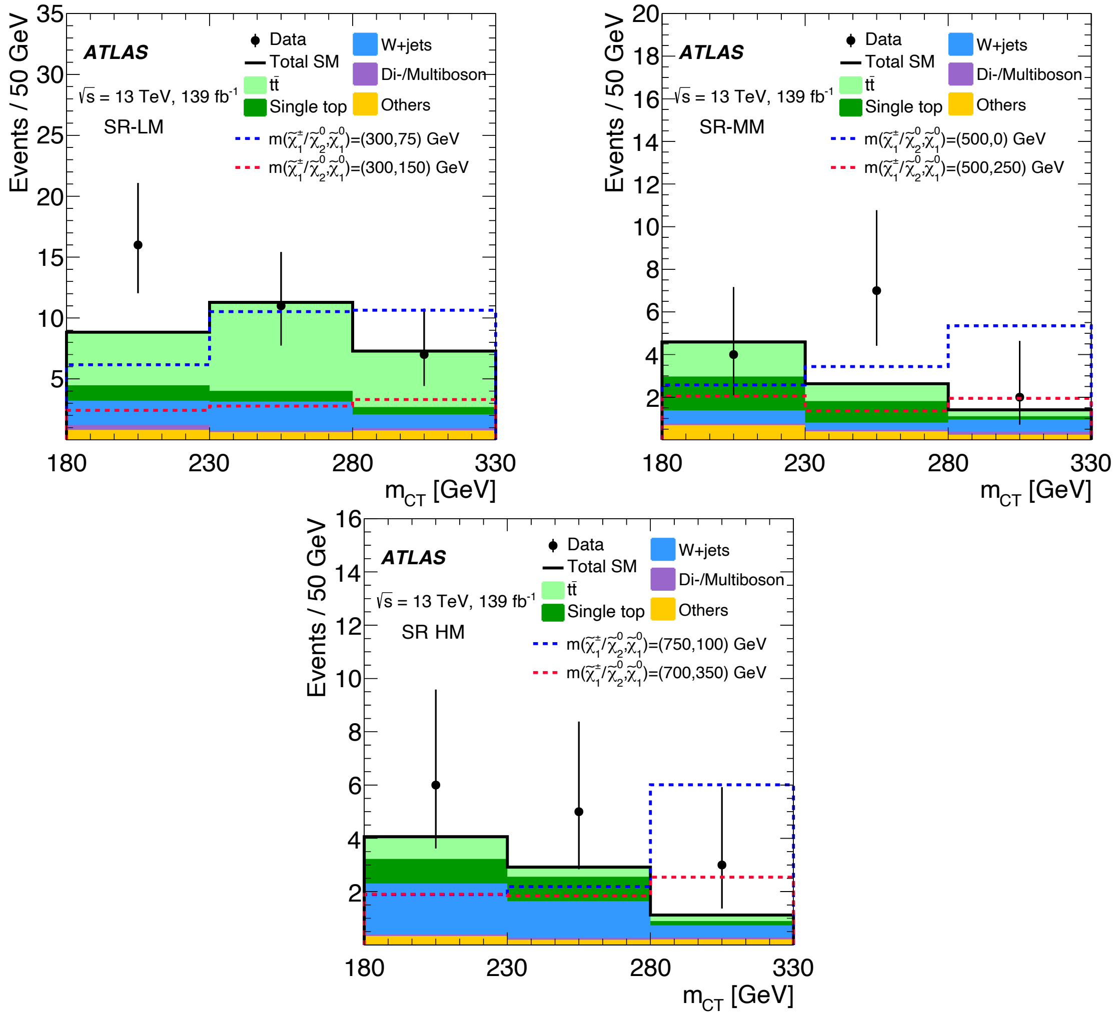

Figure 8.3: Exemplary distribution shown in each exclusion signal region after the background-only fit. The shaded region includes all systematic uncertainties (including correlations) as well as MC statistical uncertainty.

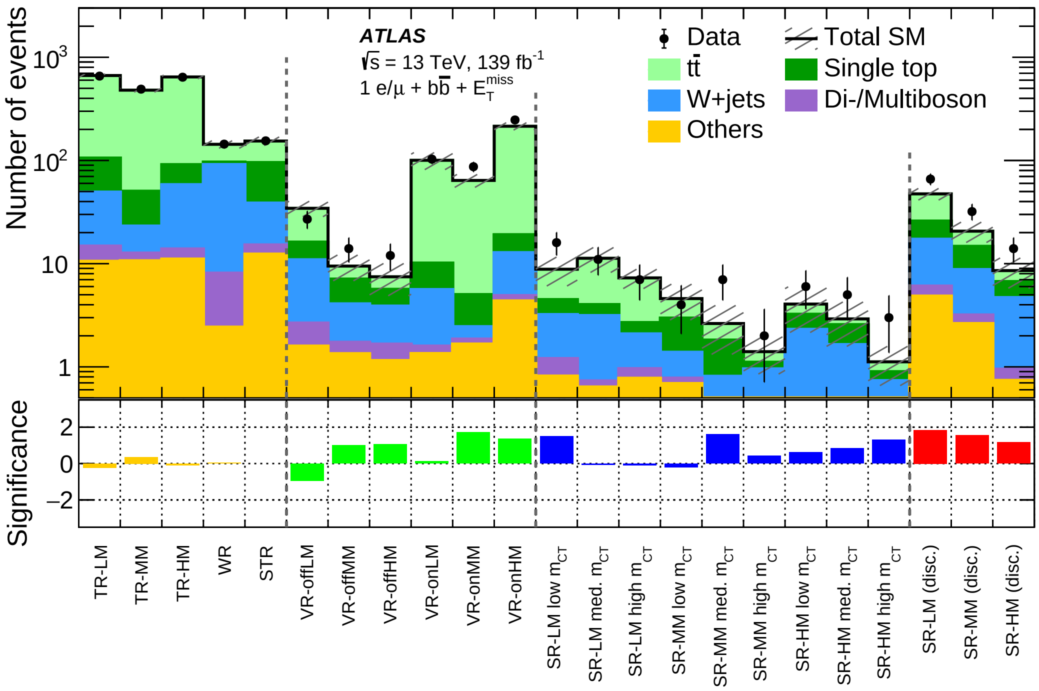

Figure 8.4

8.2 Interpretation

As no significant excess of data is observed in any of the signal regions, model-independent as well as model-dependent limits are are computed.

8.2.1 Model-independent upper limits

Model-independent upper limits on the visible cross section of new physics are derived using the discovery SRs. For this, a likelihood containing terms for the CRs and the discovery SRs is used. Since the discovery SRs are not mutually exclusive, only one discovery SR enters the likelihood at a time. This results in three distinct fit configurations in which the signal strength μ is the Parameter of Interest (POI) and no signal contamination is assumed in the control regions. The POI is subsequently scanned in distinct steps from 0 to high[†] values, followed by a hypothesis test at each scan step. The upper limit on the number of observed signal events S^{95}_{obs} is then given by the value of μ for which the corresponding CL_s value drops below 0.05. An upper limit on the visible cross section $\langle\epsilon\sigma\rangle^{95}_{\mathrm{obs}}$ is then obtained by dividing S^{95}_{obs} by the integrated luminosity of $139\,\mathrm{fb}^{-1}$. In addition to the upper limits on $\langle\epsilon\sigma\rangle^{95}_{\mathrm{obs}}$ and S^{95}_{obs}, table 8.5 also gives the p-values (and corresponding significances) for rejecting the background-only hypothesis in favour of the signal-plus-background hypothesis. As all significances are below 1.88σ for all SRs, no indication for physics beyond the SM is seen.

[†] The signal strength is in principle allowed to exceed unity in order to find an 95% CL upper limit

Table 8.5: Left to right: 95% CL upper limits on the visible cross-section ($\langle\epsilon\sigma\rangle^{95}_{\text{obs}}$) and on the number of signal events (S^{95}_{obs}). The third column (S^{95}_{exp}) shows the expected 95% CL upper limit (and its $\pm 1\sigma$ excursions) on the number of signal events if no BSM signal is present. The last three columns indicate the CL_B value, i.e. the confidence level observed for the background-only hypothesis, the discovery p-value (p_0) and the significance Z [**?**].

Signal Region	$\langle\epsilon\sigma\rangle^{95}_{\text{obs}}$[fb]	S^{95}_{obs}	S^{95}_{exp}	CL_B	p_0	Z
SR-LM (disc.)	0.26	36.8	$20.0^{+8.0}_{-5.4}$	0.97	0.03	1.88
SR-MM (disc.)	0.18	24.8	$15.3^{+6.2}_{-4.6}$	0.94	0.06	1.54
SR-HM (disc.)	0.11	14.7	$9.7^{+3.3}_{-2.7}$	0.89	0.10	1.30

8.2.2 Model-dependent exclusion limits

For each signal point in the signal grid considered, a separate *exclusion* fit is run in the CRs and the exclusion SRs. As all exclusion signal region bins are disjoint, a likelihood containing terms for all bins can be constructed, effectively creating a shape-fit in the binned variables m_T and m_CT. As opposed to the background-only fit, the exclusion fits allow for signal contribution in all regions considered, and considers the signal strength μ to be a free parameter. For each point in the signal grid, the expected and observed CL_s value is calculated as discussed in section 3.4. Expected (observed) contour lines can then be drawn at expected (observed) $\text{CL}_s = 0.05$. Signal points inside the contour are excluded at 95% CL. Figure 8.5 shows the exclusion contours obtained in the $\tilde{\chi}^\pm_1\tilde{\chi}^0_2$ signal grid considered in the analysis. The dashed line corresponds to the expected exclusion contour, obtained using the Asimov dataset. The yellow uncertainty band represents the interval containing 68% of all exclusion contours obtained for observations distributed according to the background-only hypothesis. The solid red line represents the observed exclusion limit obtained using the data recorded by ATLAS. As discussed in section 7.2.2, the dashed red lines are obtained by varying the signal cross sections up and down by 1σ.

Due to the slight overfluctuations of data observed in some of the exclusion signal region bins, the observed limit is slightly weaker than the expected one. The observed exclusion limit extends to about 740 GeV in $m(\tilde{\chi}^\pm_1/\tilde{\chi}^0_2)$ for massless $\tilde{\chi}^0_1$, and up to 600 GeV for $m(\tilde{\chi}^0_1) = 250$ GeV. This extends the previous limit set by ATLAS in this simplified model and decay channel by more than 200 GeV in $m(\tilde{\chi}^\pm_1/\tilde{\chi}^0_2)$ for massless $\tilde{\chi}^0_1$, an improvement made possible not only by the increase in integrated luminosity but also the introduction of a two-dimensional shape fit in the analysis strategy.

8.3 Discussion

At the time of writing, the limits derived in this analysis are the most stringent limits on the $\tilde{\chi}^\pm_1\tilde{\chi}^0_2 \to Wh\tilde{\chi}^0_1\tilde{\chi}^0_1$ simplified model set by an ATLAS search [239], surpassing not only the previous iteration of the analysis [**?**], but also yielding more stringent limits than those published by ATLAS in other decay channels of the same model. Figure 8.6 shows a summary of results published by ATLAS searches in the $\tilde{\chi}^\pm_1\tilde{\chi}^0_2 \to Wh\tilde{\chi}^0_1\tilde{\chi}^0_1$ simplified model. The search presented in this work is referred to as *1Lbb*. Additional searches in the 0 lepton as well as 1

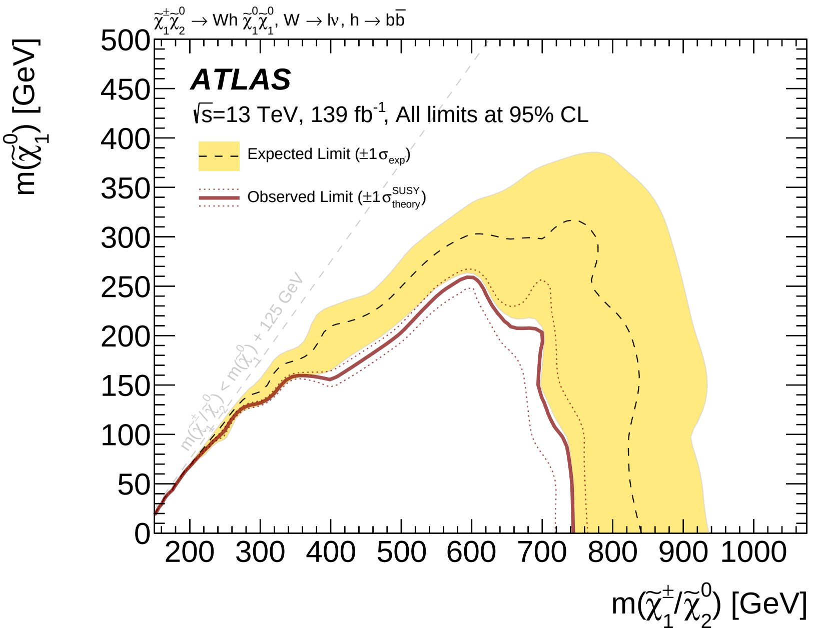

Figure 8.5

lepton final states are being worked on, and are expected to extend the limits on $m(\tilde{\chi}^{\pm}_1/\tilde{\chi}^0_2)$ up to roughly 1 TeV for massless $\tilde{\chi}^0_1$ as well as slightly extend the excluded parameter space towards the diagonal where $m(\tilde{\chi}^{\pm}_1/\tilde{\chi}^0_2) = m(\tilde{\chi}^0_1) + m(h)^{\dagger}$. cite

Various other searches for Supersymmetry (SUSY) at both ATLAS and CMS are constraining a multitude of other supersymmetric particle production and decay processes. The limits on gluino and squark pair production at the Large Hadron Collider (LHC) are particularly heavily constrained, reaching 2 TeV in many cases. With the large integrated luminosity available through the full Run 2 dataset and the improved analysis techniques and strategies developed over the last years, the typically weaker limits on electroweakinos and sleptons are also significantly increasing and in some cases approach the 1 TeV mark. The vast SUSY search program at ATLAS and CMS thus heavily constrains the existence of SUSY at the TeV scale. Still, discarding the possibility for SUSY to exist at the energies available with the LHC is much too early, for several reasons. By the end of the lifetime of the LHC (including the high luminosity upgrade HL-LHC), a projected amount of 3000 fb^{-1} [240] will have been delivered to the particle physics experiments. Many supersymmetric models not accessible with the full Run 2 dataset using today's analyses will hence only be in reach in the coming years of the LHC.

More importantly, most of the quoted limits assume simplified SUSY models and are thus only valid if the assumptions of the respective simplified model are realised in nature. In any realistic SUSY scenario that could be realised in nature and is accessible to the LHC, assumptions like 100% branching ratios or a small set of supersymmetric particles participating in the decay chains are most likely not exactly fulfilled. Thus, the quoted simplified model limits can in general not be trivially interpreted as the true underlying constraint on the respective parameter

† Assuming that no significant excess in data is seen in the search regions of these analyses.

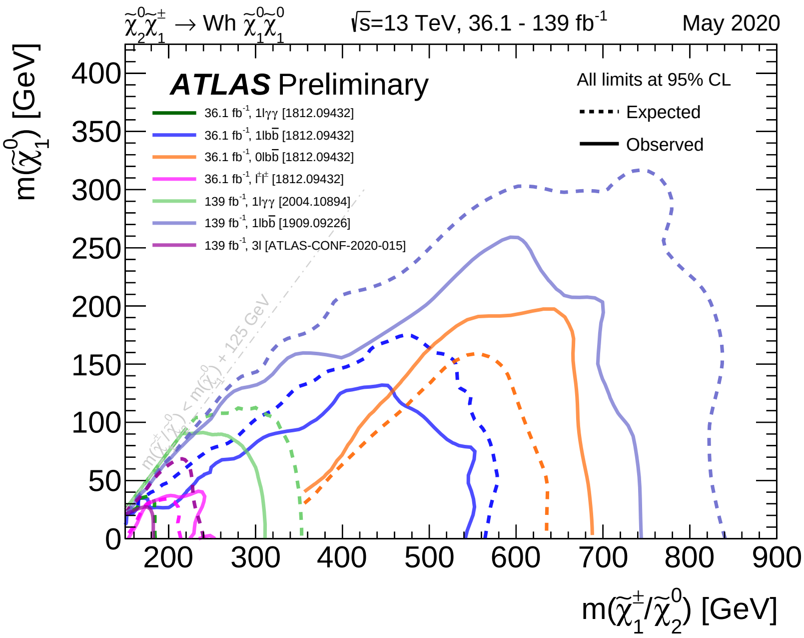

Figure 8.6

of a more realistic SUSY scenario. Due to the optimistic assumptions like 100% branching fractions, the true constraints will in general be significantly weaker than the simplified model limits. Reinterpretations of Run 1 ATLAS SUSY searches in the phenomenological Minimal Supersymmetric Standard Model (pMSSM) [76] have indeed shown that constraints on the supersymmetric masses are weaker in more complex SUSY models than those quoted for the simplified models studied in most analyses.

Naturally, there is a large interest in the high-energy physics community—both within ATLAS as well as outside of the collaboration—to perform reinterpretations of the existing SUSY searches in new, promising signal models. Compelling reasons for performing reinterpretations include, amongst others, the possibility to state a combined sensitivity of the ATLAS search program to more realistic and complex SUSY scenarios (compared to the simplified model limits). However, especially when considering high-dimensional parameter spaces like the pMSSM, such reinterpretation efficiencies quickly become extremely computationally expensive and require appropriate approximations. The following part of this work will introduce and discuss some of these approximations and show preliminary reinterpretation results of the analysis in the pMSSM.

Part III

Reinterpretation

Part IV

Summary and Outlook

Part V

Appendix

Abbreviations

CR control region. 111–113, 115, 119, 120

LHC Large Hadron Collider. 121

MC Monte Carlo. 111–118

pMSSM phenomenological Minimal Supersymmetric Standard Model. 122

POI Parameter of Interest. 119

SM Standard Model of Particle Physics. 111, 113, 115, 116, 119

SR signal region. 111, 113, 115–117, 119, 120

SUSY Supersymmetry. 121, 122

VR validation region. 111, 113–115

Bibliography

[1] I. C. Brock and T. Schorner-Sadenius, *Physics at the terascale*. Wiley, Weinheim, 2011. https://cds.cern.ch/record/1354959.

[2] M. E. Peskin and D. V. Schroeder, *An Introduction to quantum field theory*. Addison-Wesley, Reading, USA, 1995. http://www.slac.stanford.edu/~mpeskin/QFT.html.

[3] S. P. Martin, "A Supersymmetry primer," arXiv:hep-ph/9709356 [hep-ph]. [Adv. Ser. Direct. High Energy Phys.18,1(1998)].

[4] M. Bustamante, L. Cieri, and J. Ellis, "Beyond the Standard Model for Montaneros," in *5th CERN - Latin American School of High-Energy Physics*. 11, 2009. arXiv:0911.4409 [hep-ph].

[5] L. Brown, *The Birth of particle physics*. Cambridge University Press, Cambridge Cambridgeshire New York, 1986.

[6] P. J. Mohr, D. B. Newell, and B. N. Taylor, "CODATA Recommended Values of the Fundamental Physical Constants: 2014," *Rev. Mod. Phys.* **88** no. 3, (2016) 035009, arXiv:1507.07956 [physics.atom-ph].

[7] P. D. Group, "Review of Particle Physics," *Progress of Theoretical and Experimental Physics* **2020** no. 8, (08, 2020) , https://academic.oup.com/ptep/article-pdf/2020/8/083C01/34673722/ptaa104.pdf. https://doi.org/10.1093/ptep/ptaa104. 083C01.

[8] **Super-Kamiokande** Collaboration, Y. Fukuda *et al.*, "Evidence for oscillation of atmospheric neutrinos," *Phys. Rev. Lett.* **81** (1998) 1562–1567, arXiv:hep-ex/9807003 [hep-ex].

[9] Z. Maki, M. Nakagawa, and S. Sakata, "Remarks on the unified model of elementary particles," *Prog. Theor. Phys.* **28** (1962) 870–880. [,34(1962)].

[10] N. Cabibbo, "Unitary symmetry and leptonic decays," *Phys. Rev. Lett.* **10** (Jun, 1963) 531–533. https://link.aps.org/doi/10.1103/PhysRevLett.10.531.

[11] M. Kobayashi and T. Maskawa, "CP Violation in the Renormalizable Theory of Weak Interaction," *Prog. Theor. Phys.* **49** (1973) 652–657.

[12] E. Noether and M. A. Tavel, "Invariant variation problems," arXiv:physics/0503066.

[13] J. C. Ward, "An identity in quantum electrodynamics," *Phys. Rev.* **78** (Apr, 1950) 182–182. https://link.aps.org/doi/10.1103/PhysRev.78.182.

[14] Y. Takahashi, "On the generalized ward identity," *Il Nuovo Cimento (1955-1965)* **6** no. 2, (Aug, 1957) 371–375. https://doi.org/10.1007/BF02832514.

[15] G. 'tHooft, "Renormalization of massless yang-mills fields," *Nuclear Physics B* **33** no. 1, (1971) 173 – 199. http://www.sciencedirect.com/science/article/pii/0550321371903956.

[16] J. Taylor, "Ward identities and charge renormalization of the yang-mills field," *Nuclear Physics B* **33** no. 2, (1971) 436 – 444. http://www.sciencedirect.com/science/article/pii/0550321371902975.

[17] A. A. Slavnov, "Ward identities in gauge theories," *Theoretical and Mathematical Physics* **10** no. 2, (Feb, 1972) 99–104. https://doi.org/10.1007/BF01090719.

[18] C. N. Yang and R. L. Mills, "Conservation of isotopic spin and isotopic gauge invariance," *Phys. Rev.* **96** (Oct, 1954) 191–195. https://link.aps.org/doi/10.1103/PhysRev.96.191.

[19] K. G. Wilson, "Confinement of quarks," *Phys. Rev. D* **10** (Oct, 1974) 2445–2459. https://link.aps.org/doi/10.1103/PhysRevD.10.2445.

[20] T. DeGrand and C. DeTar, *Lattice Methods for Quantum Chromodynamics*. World Scientific, Singapore, 2006. https://cds.cern.ch/record/1055545.

[21] S. L. Glashow, "Partial-symmetries of weak interactions," *Nuclear Physics* **22** no. 4, (1961) 579 – 588. http://www.sciencedirect.com/science/article/pii/0029558261904692.

[22] S. Weinberg, "A model of leptons," *Phys. Rev. Lett.* **19** (Nov, 1967) 1264–1266. https://link.aps.org/doi/10.1103/PhysRevLett.19.1264.

[23] A. Salam and J. C. Ward, "Weak and electromagnetic interactions," *Il Nuovo Cimento (1955-1965)* **11** no. 4, (Feb, 1959) 568–577. https://doi.org/10.1007/BF02726525.

[24] C. S. Wu, E. Ambler, R. W. Hayward, D. D. Hoppes, and R. P. Hudson, "Experimental test of parity conservation in beta decay," *Phys. Rev.* **105** (Feb, 1957) 1413–1415. https://link.aps.org/doi/10.1103/PhysRev.105.1413.

[25] M. Gell-Mann, "The interpretation of the new particles as displaced charge multiplets," *Il Nuovo Cimento (1955-1965)* **4** no. 2, (Apr, 1956) 848–866. https://doi.org/10.1007/BF02748000.

[26] K. Nishijima, "Charge Independence Theory of V Particles*," *Progress of Theoretical Physics* **13** no. 3, (03, 1955) 285–304, `https://academic.oup.com/ptp/article-pdf/13/3/285/5425869/13-3-285.pdf`. https://doi.org/10.1143/PTP.13.285.

[27] T. Nakano and K. Nishijima, "Charge Independence for V-particles*," *Progress of Theoretical Physics* **10** no. 5, (11, 1953) 581–582, `https://academic.oup.com/ptp/article-pdf/10/5/581/5364926/10-5-581.pdf`. https://doi.org/10.1143/PTP.10.581.

[28] F. Englert and R. Brout, "Broken symmetry and the mass of gauge vector mesons," *Phys. Rev. Lett.* **13** (Aug, 1964) 321–323. https://link.aps.org/doi/10.1103/PhysRevLett.13.321.

[29] P. W. Higgs, "Broken symmetries and the masses of gauge bosons," *Phys. Rev. Lett.* **13** (Oct, 1964) 508–509. https://link.aps.org/doi/10.1103/PhysRevLett.13.508.

[30] P. W. Higgs, "Spontaneous symmetry breakdown without massless bosons," *Phys. Rev.* **145** (May, 1966) 1156–1163. https://link.aps.org/doi/10.1103/PhysRev.145.1156.

[31] Y. Nambu, "Quasiparticles and Gauge Invariance in the Theory of Superconductivity," *Phys. Rev.* **117** (1960) 648–663. [,132(1960)].

[32] J. Goldstone, "Field Theories with Superconductor Solutions," *Nuovo Cim.* **19** (1961) 154–164.

[33] V. Brdar, A. J. Helmboldt, S. Iwamoto, and K. Schmitz, "Type-I Seesaw as the Common Origin of Neutrino Mass, Baryon Asymmetry, and the Electroweak Scale," *Phys. Rev. D* **100** (2019) 075029, `arXiv:1905.12634 [hep-ph]`.

[34] G. 't Hooft and M. Veltman, "Regularization and renormalization of gauge fields," *Nuclear Physics B* **44** no. 1, (1972) 189 – 213. http://www.sciencedirect.com/science/article/pii/0550321372902799.

[35] F. Zwicky, "Die Rotverschiebung von extragalaktischen Nebeln," *Helv. Phys. Acta* **6** (1933) 110–127. https://cds.cern.ch/record/437297.

[36] V. C. Rubin and W. K. Ford, Jr., "Rotation of the Andromeda Nebula from a Spectroscopic Survey of Emission Regions," *Astrophys. J.* **159** (1970) 379–403.

[37] G. Bertone, D. Hooper, and J. Silk, "Particle dark matter: Evidence, candidates and constraints," *Phys. Rept.* **405** (2005) 279–390, `arXiv:hep-ph/0404175`.

[38] D. Clowe, M. Bradac, A. H. Gonzalez, M. Markevitch, S. W. Randall, C. Jones, and D. Zaritsky, "A direct empirical proof of the existence of dark matter," *Astrophys. J.* **648** (2006) L109–L113, `arXiv:astro-ph/0608407 [astro-ph]`.

[39] A. Taylor, S. Dye, T. J. Broadhurst, N. Benitez, and E. van Kampen, "Gravitational lens magnification and the mass of abell 1689," *Astrophys. J.* **501** (1998) 539, `arXiv:astro-ph/9801158`.

[40] C. Bennett *et al.*, "Four year COBE DMR cosmic microwave background observations: Maps and basic results," *Astrophys. J. Lett.* **464** (1996) L1–L4, `arXiv:astro-ph/9601067`.

[41] G. F. Smoot *et al.*, "Structure in the COBE Differential Microwave Radiometer First-Year Maps," *ApJS* **396** (September, 1992) L1.

[42] **WMAP** Collaboration, "Nine-year Wilkinson Microwave Anisotropy Probe (WMAP) Observations: Final Maps and Results," *ApJS* **208** no. 2, (October, 2013) 20, `arXiv:1212.5225 [astro-ph.CO]`.

[43] **WMAP** Collaboration, "Nine-year Wilkinson Microwave Anisotropy Probe (WMAP) Observations: Cosmological Parameter Results," *ApJS* **208** no. 2, (October, 2013) 19, `arXiv:1212.5226 [astro-ph.CO]`.

[44] **Planck** Collaboration, "Planck 2018 results. I. Overview and the cosmological legacy of Planck," *Astron. Astrophys.* **641** (2020) A1, `arXiv:1807.06205 [astro-ph.CO]`.

[45] A. Liddle, *An introduction to modern cosmology; 3rd ed.* Wiley, Chichester, Mar, 2015. https://cds.cern.ch/record/1976476.

[46] **Planck** Collaboration, "Planck 2018 results. VI. Cosmological parameters," *Astron. Astrophys.* **641** (2020) A6, `arXiv:1807.06209 [astro-ph.CO]`.

[47] H. Georgi and S. L. Glashow, "Unity of all elementary-particle forces," *Phys. Rev. Lett.* **32** (Feb, 1974) 438–441. https://link.aps.org/doi/10.1103/PhysRevLett.32.438.

[48] I. Aitchison, *Supersymmetry in Particle Physics. An Elementary Introduction*. Cambridge University Press, Cambridge, 2007.

[49] **Muon g-2** Collaboration, G. Bennett *et al.*, "Final Report of the Muon E821 Anomalous Magnetic Moment Measurement at BNL," *Phys. Rev. D* **73** (2006) 072003, arXiv:hep-ex/0602035.

[50] H. Baer and X. Tata, *Weak Scale Supersymmetry: From Superfields to Scattering Events*. Cambridge University Press, 2006.

[51] A. Czarnecki and W. J. Marciano, "The Muon anomalous magnetic moment: A Harbinger for 'new physics'," *Phys. Rev. D* **64** (2001) 013014, arXiv:hep-ph/0102122.

[52] J. L. Feng and K. T. Matchev, "Supersymmetry and the anomalous magnetic moment of the muon," *Phys. Rev. Lett.* **86** (2001) 3480–3483, arXiv:hep-ph/0102146.

[53] S. Coleman and J. Mandula, "All possible symmetries of the s matrix," *Phys. Rev.* **159** (Jul, 1967) 1251–1256. https://link.aps.org/doi/10.1103/PhysRev.159.1251.

[54] R. Haag, J. T. Lopuszanski, and M. Sohnius, "All Possible Generators of Supersymmetries of the s Matrix," *Nucl. Phys.* **B88** (1975) 257. [,257(1974)].

[55] J. Wess and B. Zumino, "Supergauge transformations in four dimensions," *Nuclear Physics B* **70** no. 1, (1974) 39 – 50. http://www.sciencedirect.com/science/article/pii/0550321374903551.

[56] H. Georgi and S. L. Glashow, "Gauge theories without anomalies," *Phys. Rev. D* **6** (Jul, 1972) 429–431. https://link.aps.org/doi/10.1103/PhysRevD.6.429.

[57] S. Dimopoulos and D. W. Sutter, "The Supersymmetric flavor problem," *Nucl. Phys. B* **452** (1995) 496–512, arXiv:hep-ph/9504415.

[58] **MEG** Collaboration, T. Mori, "Final Results of the MEG Experiment," *Nuovo Cim. C* **39** no. 4, (2017) 325, arXiv:1606.08168 [hep-ex].

[59] H. P. Nilles, "Supersymmetry, Supergravity and Particle Physics," *Phys. Rept.* **110** (1984) 1–162.

[60] A. Lahanas and D. Nanopoulos, "The road to no-scale supergravity," *Physics Reports* **145** no. 1, (1987) 1 – 139. http://www.sciencedirect.com/science/article/pii/0370157387900342.

[61] J. L. Feng, A. Rajaraman, and F. Takayama, "Superweakly interacting massive particles," *Phys. Rev. Lett.* **91** (2003) 011302, arXiv:hep-ph/0302215.

[62] **Super-Kamiokande** Collaboration, K. Abe *et al.*, "Search for proton decay via $p \to e^+\pi^0$ and $p \to \mu^+\pi^0$ in 0.31 megaton-years exposure of the Super-Kamiokande water Cherenkov detector," *Phys. Rev.* **D95** no. 1, (2017) 012004, arXiv:1610.03597 [hep-ex].

[63] J. R. Ellis, "Beyond the standard model for hill walkers," in *1998 European School of High-Energy Physics*, pp. 133–196. 8, 1998. arXiv:hep-ph/9812235.

[64] J. R. Ellis, J. Hagelin, D. V. Nanopoulos, K. A. Olive, and M. Srednicki, "Supersymmetric Relics from the Big Bang," *Nucl. Phys. B* **238** (1984) 453–476.

[65] D. O. Caldwell, R. M. Eisberg, D. M. Grumm, M. S. Witherell, B. Sadoulet, F. S. Goulding, and A. R. Smith, "Laboratory limits on galactic cold dark matter," *Phys. Rev. Lett.* **61** (Aug, 1988) 510–513. https://link.aps.org/doi/10.1103/PhysRevLett.61.510.

[66] M. Mori, M. M. Nojiri, K. S. Hirata, K. Kihara, Y. Oyama, A. Suzuki, K. Takahashi, M. Yamada, H. Takei, M. Koga, K. Miyano, H. Miyata, Y. Fukuda, T. Hayakawa, K. Inoue, T. Ishida, T. Kajita, Y. Koshio, M. Nakahata, K. Nakamura, A. Sakai, N. Sato, M. Shiozawa, J. Suzuki, Y. Suzuki, Y. Totsuka, M. Koshiba, K. Nishijima, T. Kajimura, T. Suda, A. T. Suzuki, T. Hara, Y. Nagashima, M. Takita, H. Yokoyama, A. Yoshimoto, K. Kaneyuki, Y. Takeuchi, T. Tanimori, S. Tasaka, and K. Nishikawa, "Search for neutralino dark matter heavier than the w boson at kamiokande," *Phys. Rev. D* **48** (Dec, 1993) 5505–5518. https://link.aps.org/doi/10.1103/PhysRevD.48.5505.

[67] **CDMS** Collaboration, D. S. Akerib *et al.*, "Exclusion limits on the WIMP-nucleon cross section from the first run of the Cryogenic Dark Matter Search in the Soudan Underground Laboratory," *Phys. Rev. D* **72** (2005) 052009, `arXiv:astro-ph/0507190`.

[68] A. Djouadi, J.-L. Kneur, and G. Moultaka, "SuSpect: A Fortran code for the supersymmetric and Higgs particle spectrum in the MSSM," *Comput. Phys. Commun.* **176** (2007) 426–455, `arXiv:hep-ph/0211331`.

[69] C. F. Berger, J. S. Gainer, J. L. Hewett, and T. G. Rizzo, "Supersymmetry without prejudice," *Journal of High Energy Physics* **2009** no. 02, (Feb, 2009) 023–023. http://dx.doi.org/10.1088/1126-6708/2009/02/023.

[70] J. Alwall, P. Schuster, and N. Toro, "Simplified Models for a First Characterization of New Physics at the LHC," *Phys. Rev.* **D79** (2009) 075020, `arXiv:0810.3921 [hep-ph]`.

[71] **LHC New Physics Working Group** Collaboration, D. Alves, "Simplified Models for LHC New Physics Searches," *J. Phys.* **G39** (2012) 105005, `arXiv:1105.2838 [hep-ph]`.

[72] D. S. Alves, E. Izaguirre, and J. G. Wacker, "Where the Sidewalk Ends: Jets and Missing Energy Search Strategies for the 7 TeV LHC," *JHEP* **10** (2011) 012, `arXiv:1102.5338 [hep-ph]`.

[73] F. Ambrogi, S. Kraml, S. Kulkarni, U. Laa, A. Lessa, and W. Waltenberger, "On the coverage of the pMSSM by simplified model results," *Eur. Phys. J. C* **78** no. 3, (2018) 215, `arXiv:1707.09036 [hep-ph]`.

[74] O. Buchmueller and J. Marrouche, "Universal mass limits on gluino and third-generation squarks in the context of Natural-like SUSY spectra," *Int. J. Mod. Phys. A* **29** no. 06, (2014) 1450032, `arXiv:1304.2185 [hep-ph]`.

[75] **ATLAS** Collaboration, M. Aaboud *et al.*, "Dark matter interpretations of ATLAS searches for the electroweak production of supersymmetric particles in $\sqrt{s} = 8$ TeV proton-proton collisions," *JHEP* **09** (2016) 175, `arXiv:1608.00872 [hep-ex]`.

[76] **ATLAS** Collaboration, "Summary of the ATLAS experiment's sensitivity to supersymmetry after LHC Run 1 — interpreted in the phenomenological MSSM," *JHEP* **10** (2015) 134, `arXiv:1508.06608 [hep-ex]`.

[77] **ATLAS** Collaboration, "Mass reach of the atlas searches for supersymmetry." https://atlas.web.cern.ch/Atlas/GROUPS/PHYSICS/PUBNOTES/ATL-PHYS-PUB-2020-020/fig_23.png, 2020.

[78] **CMS** Collaboration, "Summary plot moriond 2017." https://twiki.cern.ch/twiki/pub/CMSPublic/SUSYSummary2017/Moriond2017_BarPlot.pdf, 2017.

[79] L. S. W. Group, "Notes lepsusywg/02-04.1 and lepsusywg/01-03.1." http://lepsusy.web.cern.ch/lepsusy/, 2004. Accessed: 2021-02-11.

[80] **ATLAS** Collaboration, G. Aad *et al.*, "Observation of a new particle in the search for the Standard Model Higgs boson with the ATLAS detector at the LHC," *Phys. Lett. B* **716** (2012) 1–29, `arXiv:1207.7214 [hep-ex]`.

[81] **CMS** Collaboration, S. Chatrchyan *et al.*, "Observation of a New Boson at a Mass of 125 GeV with the CMS Experiment at the LHC," *Phys. Lett. B* **716** (2012) 30–61, `arXiv:1207.7235 [hep-ex]`.

[82] CERN, "About cern." https://home.cern/about. Accessed: 2021-01-21.

[83] CERN, "CERN Annual report 2019," tech. rep., CERN, Geneva, 2020. https://cds.cern.ch/record/2723123.

[84] L. R. Evans and P. Bryant, "LHC Machine," *JINST* **3** (2008) S08001. 164 p. http://cds.cern.ch/record/1129806. This report is an abridged version of the LHC Design Report (CERN-2004-003).

[85] R. Scrivens, M. Kronberger, D. Küchler, J. Lettry, C. Mastrostefano, O. Midttun, M. O'Neil, H. Pereira, and C. Schmitzer, "Overview of the status and developments on primary ion sources at CERN*,". https://cds.cern.ch/record/1382102.

[86] E. Mobs, "The CERN accelerator complex - 2019. Complexe des accélérateurs du CERN - 2019,". https://cds.cern.ch/record/2684277. General Photo.

[87] **ATLAS** Collaboration, "The ATLAS Experiment at the CERN Large Hadron Collider," *JINST* **3** (2008) S08003.

[88] **CMS** Collaboration, S. Chatrchyan *et al.*, "The CMS Experiment at the CERN LHC," *JINST* **3** (2008) S08004.

[89] **ALICE** Collaboration, K. Aamodt *et al.*, "The ALICE experiment at the CERN LHC," *JINST* **3** (2008) S08002.

[90] **LHCb** Collaboration, J. Alves, A.Augusto *et al.*, "The LHCb Detector at the LHC," *JINST* **3** (2008) S08005.

[91] **TOTEM** Collaboration, G. Anelli *et al.*, "The TOTEM experiment at the CERN Large Hadron Collider," *JINST* **3** (2008) S08007.

[92] **LHCf** Collaboration, O. Adriani *et al.*, "Technical design report of the LHCf experiment: Measurement of photons and neutral pions in the very forward region of LHC,".

[93] **MoEDAL** Collaboration, J. Pinfold *et al.*, "Technical Design Report of the MoEDAL Experiment,".

[94] O. S. Bruning, P. Collier, P. Lebrun, S. Myers, R. Ostojic, J. Poole, and P. Proudlock, *LHC Design Report*. CERN Yellow Reports: Monographs. CERN, Geneva, 2004. https://cds.cern.ch/record/782076.

[95] **ATLAS** Collaboration, "ATLAS Public Results - Luminosity Public Results Run 2,". https://twiki.cern.ch/twiki/bin/view/AtlasPublic/LuminosityPublicResultsRun2. Accessed: 2021-01-17.

[96] **ATLAS** Collaboration, Z. Marshall, "Simulation of Pile-up in the ATLAS Experiment," *J. Phys. Conf. Ser.* **513** (2014) 022024.

[97] "First beam in the LHC - accelerating science,". https://home.cern/news/news/accelerators/record-luminosity-well-done-lhc. Accessed: 2021-01-10.

[98] **ATLAS Collaboration** Collaboration, "Luminosity determination in *pp* collisions at $\sqrt{s} = 13$ TeV using the ATLAS detector at the LHC," Tech. Rep. ATLAS-CONF-2019-021, CERN, Geneva, Jun, 2019. https://cds.cern.ch/record/2677054.

[99] **ATLAS** Collaboration, M. Aaboud *et al.*, "Luminosity determination in pp collisions at $\sqrt{s} = 8$ TeV using the ATLAS detector at the LHC," *Eur. Phys. J. C* **76** no. 12, (2016) 653, arXiv:1608.03953 [hep-ex].

[100] G. Avoni, M. Bruschi, G. Cabras, D. Caforio, N. Dehghanian, A. Floderus, B. Giacobbe, F. Giannuzzi, F. Giorgi, P. Grafström, V. Hedberg, F. L. Manghi, S. Meneghini, J. Pinfold, E. Richards, C. Sbarra, N. S. Cesari, A. Sbrizzi, R. Soluk, G. Ucchielli, S. Valentinetti, O. Viazlo, M. Villa, C. Vittori, R. Vuillermet, and A. Zoccoli, "The new LUCID-2 detector for luminosity measurement and monitoring in ATLAS," *Journal of Instrumentation* **13** no. 07, (Jul, 2018) P07017–P07017. https://doi.org/10.1088/1748-0221/13/07/p07017.

[101] S. van der Meer, "Calibration of the effective beam height in the ISR," Tech. Rep. CERN-ISR-PO-68-31. ISR-PO-68-31, CERN, Geneva, 1968. https://cds.cern.ch/record/296752.

[102] P. Grafström and W. Kozanecki, "Luminosity determination at proton colliders," *Progress in Particle and Nuclear Physics* **81** (2015) 97 – 148. http://www.sciencedirect.com/science/article/pii/S0146641014000878.

[103] "New schedule for CERN's accelerators and experiments,". https://home.cern/news/press-release/cern/first-beam-lhc-accelerating-science. Accessed: 2021-01-10.

[104] **ATLAS** Collaboration, G. Aad *et al.*, "Luminosity Determination in *pp* Collisions at $\sqrt{s} = 7$ TeV Using the ATLAS Detector at the LHC," *Eur. Phys. J. C* **71** (2011) 1630, arXiv:1101.2185 [hep-ex].

[105] **ATLAS Collaboration** Collaboration, G. Aad *et al.*, "Improved luminosity determination in pp collisions at $\sqrt{s} = 7$ TeV using the ATLAS detector at the LHC. Improved luminosity determination in pp collisions at sqrt(s) = 7 TeV using the ATLAS detector at the LHC," *Eur. Phys. J. C* **73** no. CERN-PH-EP-2013-026. CERN-PH-EP-2013-026, (Feb, 2013) 2518. 27 p. https://cds.cern.ch/record/1517411. Comments: 26 pages plus author list (39 pages total), 17 figures, 9 tables, submitted to EPJC, All figures are available at <a href=.

[106] "Record luminosity: well done LHC,". https://home.cern/news/news/accelerators/new-schedule-cerns-accelerators-and-experiments. Accessed: 2021-01-10.

[107] A. G., B. A. I., B. O., F. P., L. M., R. L., and T. L., *High-Luminosity Large Hadron Collider (HL-LHC): Technical Design Report V. 0.1*. CERN Yellow Reports: Monographs. CERN, Geneva, 2017. https://cds.cern.ch/record/2284929.

[108] J. Pequenao, "Computer generated image of the whole ATLAS detector." Mar, 2008.

[109] **ATLAS** Collaboration, "ATLAS: Detector and physics performance technical design report. Volume 1,".

[110] J. Pequenao, "Computer generated image of the ATLAS inner detector." Mar, 2008.

[111] **ATLAS Collaboration** Collaboration, K. Potamianos, "The upgraded Pixel detector and the commissioning of the Inner Detector tracking of the ATLAS experiment for Run-2 at the Large Hadron Collider," Tech. Rep. ATL-PHYS-PROC-2016-104, CERN, Geneva, Aug, 2016. https://cds.cern.ch/record/2209070. 15 pages, EPS-HEP 2015 Proceedings.

[112] **ATLAS IBL** Collaboration, B. Abbott *et al.*, "Production and Integration of the ATLAS Insertable B-Layer," *JINST* **13** no. 05, (2018) T05008, `arXiv:1803.00844 [physics.ins-det]`.

[113] **ATLAS** Collaboration, "ATLAS Insertable B-Layer Technical Design Report," Tech. Rep. CERN-LHCC-2010-013. ATLAS-TDR-19, Sep, 2010. http://cds.cern.ch/record/1291633.

[114] **ATLAS** Collaboration, G. Aad *et al.*, "ATLAS b-jet identification performance and efficiency measurement with $t\bar{t}$ events in pp collisions at $\sqrt{s} = 13$ TeV," *Eur. Phys. J. C* **79** no. 11, (2019) 970, `arXiv:1907.05120 [hep-ex]`.

[115] ATLAS Collaboration, "Particle Identification Performance of the ATLAS Transition Radiation Tracker." ATLAS-CONF-2011-128, 2011. https://cds.cern.ch/record/1383793.

[116] J. Pequenao, "Computer Generated image of the ATLAS calorimeter." Mar, 2008.

[117] J. Pequenao, "Computer generated image of the ATLAS Muons subsystem." Mar, 2008.

[118] S. Lee, M. Livan, and R. Wigmans, "Dual-Readout Calorimetry," *Rev. Mod. Phys.* **90** no. arXiv:1712.05494. 2, (Dec, 2017) 025002. 40 p. https://cds.cern.ch/record/2637852. 44 pages, 53 figures, accepted for publication in Review of Modern Physics.

[119] M. Leite, "Performance of the ATLAS Zero Degree Calorimeter," Tech. Rep. ATL-FWD-PROC-2013-001, CERN, Geneva, Nov, 2013. https://cds.cern.ch/record/1628749.

[120] S. Abdel Khalek *et al.*, "The ALFA Roman Pot Detectors of ATLAS," *JINST* **11** no. 11, (2016) P11013, `arXiv:1609.00249 [physics.ins-det]`.

[121] U. Amaldi, G. Cocconi, A. Diddens, R. Dobinson, J. Dorenbosch, W. Duinker, D. Gustavson, J. Meyer, K. Potter, A. Wetherell, A. Baroncelli, and C. Bosio, "The real part of the forward proton proton scattering amplitude measured at the cern intersecting storage rings," *Physics Letters B* **66** no. 4, (1977) 390 – 394. http://www.sciencedirect.com/science/article/pii/0370269377900223.

[122] L. Adamczyk, E. Banaś, A. Brandt, M. Bruschi, S. Grinstein, J. Lange, M. Rijssenbeek, P. Sicho, R. Staszewski, T. Sykora, M. Trzebiński, J. Chwastowski, and K. Korcyl, "Technical Design Report for the ATLAS Forward Proton Detector," Tech. Rep. CERN-LHCC-2015-009. ATLAS-TDR-024, May, 2015. https://cds.cern.ch/record/2017378.

[123] **ATLAS** Collaboration, A. R. Martínez, "The Run-2 ATLAS Trigger System," *J. Phys. Conf. Ser.* **762** no. 1, (2016) 012003.

[124] **ATLAS Collaboration** Collaboration, *ATLAS level-1 trigger: Technical Design Report*. Technical Design Report ATLAS. CERN, Geneva, 1998. https://cds.cern.ch/record/381429.

[125] **ATLAS Collaboration** Collaboration, P. Jenni, M. Nessi, M. Nordberg, and K. Smith, *ATLAS high-level trigger, data-acquisition and controls: Technical Design Report*. Technical Design Report ATLAS. CERN, Geneva, 2003. https://cds.cern.ch/record/616089.

[126] **ATLAS** Collaboration, G. Aad *et al.*, "The ATLAS Simulation Infrastructure," *Eur. Phys. J. C* **70** (2010) 823–874, arXiv:1005.4568 [physics.ins-det].

[127] T. Gleisberg, S. Hoeche, F. Krauss, M. Schonherr, S. Schumann, F. Siegert, and J. Winter, "Event generation with SHERPA 1.1," *JHEP* **02** (2009) 007, arXiv:0811.4622 [hep-ph].

[128] A. Buckley *et al.*, "General-purpose event generators for LHC physics," *Phys. Rept.* **504** (2011) 145–233, arXiv:1101.2599 [hep-ph].

[129] V. N. Gribov and L. N. Lipatov, "Deep inelastic e p scattering in perturbation theory," *Sov. J. Nucl. Phys.* **15** (1972) 438–450.

[130] J. Blumlein, T. Doyle, F. Hautmann, M. Klein, and A. Vogt, "Structure functions in deep inelastic scattering at HERA," in *Workshop on Future Physics at HERA (To be followed by meetings 7-9 Feb and 30-31 May 1996 at DESY)*. 9, 1996. arXiv:hep-ph/9609425.

[131] A. Buckley, J. Ferrando, S. Lloyd, K. Nordström, B. Page, M. Rüfenacht, M. Schönherr, and G. Watt, "LHAPDF6: parton density access in the LHC precision era," *Eur. Phys. J. C* **75** (2015) 132, arXiv:1412.7420 [hep-ph].

[132] M. Bengtsson and T. Sjostrand, "Coherent Parton Showers Versus Matrix Elements: Implications of PETRA - PEP Data," *Phys. Lett. B* **185** (1987) 435.

[133] S. Catani, F. Krauss, R. Kuhn, and B. R. Webber, "QCD matrix elements + parton showers," *JHEP* **11** (2001) 063, arXiv:hep-ph/0109231.

[134] L. Lonnblad, "Correcting the color dipole cascade model with fixed order matrix elements," *JHEP* **05** (2002) 046, arXiv:hep-ph/0112284.

[135] B. Andersson, G. Gustafson, G. Ingelman, and T. Sjostrand, "Parton Fragmentation and String Dynamics," *Phys. Rept.* **97** (1983) 31–145.

[136] B. Andersson, *The Lund Model*. Cambridge Monographs on Particle Physics, Nuclear Physics and Cosmology. Cambridge University Press, 1998.

[137] D. Amati and G. Veneziano, "Preconfinement as a Property of Perturbative QCD," *Phys. Lett. B* **83** (1979) 87–92.

[138] M. Dobbs and J. B. Hansen, "The HepMC C++ Monte Carlo event record for High Energy Physics," *Comput. Phys. Commun.* **134** (2001) 41–46.

[139] **GEANT4** Collaboration, S. Agostinelli *et al.*, "GEANT4: A Simulation toolkit," *Nucl. Instrum. Meth.* **A506** (2003) 250–303.

[140] **ATLAS Collaboration** Collaboration, "The new Fast Calorimeter Simulation in ATLAS," Tech. Rep. ATL-SOFT-PUB-2018-002, CERN, Geneva, Jul, 2018. https://cds.cern.ch/record/2630434.

[141] K. Cranmer, "Practical Statistics for the LHC," in *2011 European School of High-Energy Physics*, pp. 267–308. 2014. arXiv:1503.07622 [physics.data-an].

[142] G. Cowan, K. Cranmer, E. Gross, and O. Vitells, "Asymptotic formulae for likelihood-based tests of new physics," *Eur. Phys. J.* **C71** (2011) 1554, arXiv:1007.1727 [physics.data-an]. [Erratum: Eur. Phys. J.C73,2501(2013)].

[143] ATLAS Collaboration, "Reproduction searches for new physics with the ATLAS experiment through publication of full statistical likelihoods." ATL-PHYS-PUB-2019-029, 2019. https://cds.cern.ch/record/2684863.

[144] **ROOT Collaboration** Collaboration, K. Cranmer, G. Lewis, L. Moneta, A. Shibata, and W. Verkerke, "HistFactory: A tool for creating statistical models for use with RooFit and RooStats," Tech. Rep. CERN-OPEN-2012-016, New York U., New York, Jan, 2012. https://cds.cern.ch/record/1456844.

[145] W. Verkerke and D. P. Kirkby, "The RooFit toolkit for data modeling," *eConf* **C0303241** (2003) MOLT007, arXiv:physics/0306116 [physics]. [,186(2003)].

[146] L. Moneta, K. Belasco, K. S. Cranmer, S. Kreiss, A. Lazzaro, D. Piparo, G. Schott, W. Verkerke, and M. Wolf, "The RooStats Project," *PoS* **ACAT2010** (2010) 057, arXiv:1009.1003 [physics.data-an].

[147] F. James and M. Roos, "MINUIT: a system for function minimization and analysis of the parameter errors and corrections," *Comput. Phys. Commun.* **10** no. CERN-DD-75-20, (Jul, 1975) 343–367. 38 p. https://cds.cern.ch/record/310399.

[148] R. Brun and F. Rademakers, "ROOT: An object oriented data analysis framework," *Nucl. Instrum. Meth.* **A389** (1997) 81–86.

[149] I. Antcheva *et al.*, "Root — a c++ framework for petabyte data storage, statistical analysis and visualization," *Computer Physics Communications* **182** no. 6, (2011) 1384 – 1385. http://www.sciencedirect.com/science/article/pii/S0010465511000701.

[150] M. Baak, G. J. Besjes, D. Côte, A. Koutsman, J. Lorenz, and D. Short, "HistFitter software framework for statistical data analysis," *Eur. Phys. J.* **C75** (2015) 153, arXiv:1410.1280 [hep-ex].

[151] L. Heinrich, M. Feickert, G. Stark, and K. Cranmer, "pyhf: pure-python implementation of histfactory statistical models," *Journal of Open Source Software* **6** no. 58, (2021) 2823. https://doi.org/10.21105/joss.02823.

[152] L. Heinrich, M. Feickert, and G. Stark, "pyhf: v0.6.0." https://github.com/scikit-hep/pyhf.

[153] A. Paszke, S. Gross, F. Massa, A. Lerer, J. Bradbury, G. Chanan, T. Killeen, Z. Lin, N. Gimelshein, L. Antiga, A. Desmaison, A. Kopf, E. Yang, Z. DeVito, M. Raison, A. Tejani, S. Chilamkurthy, B. Steiner, L. Fang, J. Bai, and S. Chintala, "Pytorch: An imperative style, high-performance deep learning library," in *Advances in Neural Information Processing Systems 32*, H. Wallach, H. Larochelle, A. Beygelzimer, F. d'Alché-Buc, E. Fox, and R. Garnett, eds., pp. 8024–8035. Curran Associates, Inc., 2019. http://papers.neurips.cc/paper/9015-pytorch-an-imperative-style-high-performance-deep-learning-library.pdf.

[154] M. Abadi, A. Agarwal, P. Barham, E. Brevdo, Z. Chen, C. Citro, G. S. Corrado, A. Davis, J. Dean, M. Devin, S. Ghemawat, I. Goodfellow, A. Harp, G. Irving, M. Isard, Y. Jia, R. Jozefowicz, L. Kaiser, M. Kudlur, J. Levenberg, D. Mané, R. Monga, S. Moore, D. Murray, C. Olah, M. Schuster, J. Shlens, B. Steiner, I. Sutskever, K. Talwar, P. Tucker, V. Vanhoucke, V. Vasudevan, F. Viégas, O. Vinyals, P. Warden, M. Wattenberg, M. Wicke, Y. Yu, and X. Zheng, "TensorFlow: Large-scale machine learning on heterogeneous systems," 2015. https://www.tensorflow.org/. Software available from tensorflow.org.

[155] J. Bradbury, R. Frostig, P. Hawkins, M. J. Johnson, C. Leary, D. Maclaurin, and S. Wanderman-Milne, "JAX: composable transformations of Python+NumPy programs," 2018. http://github.com/google/jax.

[156] A. Wald, "Tests of statistical hypotheses concerning several parameters when the number of observations is large," *Transactions of the American Mathematical Society* **54** no. 3, (1943) 426–482. https://doi.org/10.1090/S0002-9947-1943-0012401-3.

[157] S. S. Wilks, "The large-sample distribution of the likelihood ratio for testing composite hypotheses," *Ann. Math. Statist.* **9** no. 1, (03, 1938) 60–62. https://doi.org/10.1214/aoms/1177732360.

[158] G. Cowan, "Statistics for Searches at the LHC," in *69th Scottish Universities Summer School in Physics: LHC Physics*, pp. 321–355. 7, 2013. arXiv:1307.2487 [hep-ex].

[159] A. L. Read, "Presentation of search results: the CL_S technique," *J. Phys. G* **28** (2002) 2693.

[160] R. D. Cousins, J. T. Linnemann, and J. Tucker, "Evaluation of three methods for calculating statistical significance when incorporating a systematic uncertainty into a test of the background-only hypothesis for a Poisson process," *Nucl. Instrum. Meth. A* **595** no. 2, (2008) 480, arXiv:physics/0702156 [physics.data-an].

[161] K. CRANMER, "Statistical challenges for searches for new physics at the lhc," *Statistical Problems in Particle Physics, Astrophysics and Cosmology* (May, 2006) . http://dx.doi.org/10.1142/9781860948985_0026.

[162] ATLAS Collaboration, "Search for direct pair production of a chargino and a neutralino decaying to the 125 GeV Higgs boson in $\sqrt{s} = 8$ TeV pp collisions with the ATLAS detector," *Eur. Phys. J. C* **75** (2015) 208, arXiv:1501.07110 [hep-ex].

[163] ATLAS Collaboration, "Search for chargino and neutralino production in final states with a Higgs boson and missing transverse momentum at $\sqrt{s} = 13$ TeV with the ATLAS detector," *Phys. Rev. D* **100** (2019) 012006, arXiv:1812.09432 [hep-ex].

[164] CMS Collaboration, "Search for electroweak production of charginos and neutralinos in WH events in proton–proton collisions at $\sqrt{s} = 13$ TeV," *JHEP* **11** (2017) 029, arXiv:1706.09933 [hep-ex].

[165] ATLAS Collaboration, “Search for direct production of electroweakinos in final states with one lepton, missing transverse momentum and a Higgs boson decaying into two b-jets in pp collisions at $\sqrt{s} = 13$ TeV with the ATLAS detector,” *Eur. Phys. J. C* **80** (2020) 691, arXiv:1909.09226 [hep-ex].

[166] ATLAS Collaboration, “Improvements in $t\bar{t}$ modelling using NLO+PS Monte Carlo generators for Run 2.” ATL-PHYS-PUB-2018-009, 2018. https://cds.cern.ch/record/2630327.

[167] ATLAS Collaboration, “Modelling of the $t\bar{t}H$ and $t\bar{t}V (V = W, Z)$ processes for $\sqrt{s} = 13$ TeV ATLAS analyses.” ATL-PHYS-PUB-2016-005, 2016. https://cds.cern.ch/record/2120826.

[168] ATLAS Collaboration, “ATLAS simulation of boson plus jets processes in Run 2.” ATL-PHYS-PUB-2017-006, 2017. https://cds.cern.ch/record/2261937.

[169] ATLAS Collaboration, “Multi-Boson Simulation for 13 TeV ATLAS Analyses.” ATL-PHYS-PUB-2017-005, 2017. https://cds.cern.ch/record/2261933.

[170] J. Alwall, R. Frederix, S. Frixione, V. Hirschi, F. Maltoni, O. Mattelaer, H. S. Shao, T. Stelzer, P. Torrielli, and M. Zaro, “The automated computation of tree-level and next-to-leading order differential cross sections, and their matching to parton shower simulations,” *JHEP* **07** (2014) 079, arXiv:1405.0301 [hep-ph].

[171] R. Frederix and S. Frixione, “Merging meets matching in MC@NLO,” *JHEP* **12** (2012) 061, arXiv:1209.6215 [hep-ph].

[172] T. Sjöstrand, S. Ask, J. R. Christiansen, R. Corke, N. Desai, P. Ilten, S. Mrenna, S. Prestel, C. O. Rasmussen, and P. Z. Skands, “An Introduction to PYTHIA 8.2,” *Comput. Phys. Commun.* **191** (2015) 159–177, arXiv:1410.3012 [hep-ph].

[173] L. Lönnblad and S. Prestel, “Matching tree-level matrix elements with interleaved showers,” *JHEP* **03** (2012) 019, arXiv:1109.4829 [hep-ph].

[174] R. D. Ball *et al.*, “Parton distributions with LHC data,” *Nucl. Phys. B* **867** (2013) 244, arXiv:1207.1303 [hep-ph].

[175] ATLAS Collaboration, “ATLAS Pythia 8 tunes to 7 TeV data.” ATL-PHYS-PUB-2014-021, 2014. https://cds.cern.ch/record/1966419.

[176] D. J. Lange, “The EvtGen particle decay simulation package,” *Nucl. Instrum. Meth. A* **462** (2001) 152.

[177] ATLAS Collaboration, “The Pythia 8 A3 tune description of ATLAS minimum bias and inelastic measurements incorporating the Donnachie–Landshoff diffractive model.” ATL-PHYS-PUB-2016-017, 2016. https://cds.cern.ch/record/2206965.

[178] B. Fuks, M. Klasen, D. R. Lamprea, and M. Rothering, “Precision predictions for electroweak superpartner production at hadron colliders with RESUMMINO,” *Eur. Phys. J. C* **73** (2013) 2480, arXiv:1304.0790 [hep-ph].

[179] J. Fiaschi and M. Klasen, “Neutralino-chargino pair production at NLO+NLL with resummation-improved parton density functions for LHC Run II,” *Phys. Rev. D* **98** no. 5, (2018) 055014, arXiv:1805.11322 [hep-ph].

[180] B. Fuks, M. Klasen, D. R. Lamprea, and M. Rothering, "Gaugino production in proton-proton collisions at a center-of-mass energy of 8 TeV," *JHEP* **10** (2012) 081, arXiv:1207.2159 [hep-ph].

[181] S. Alioli, P. Nason, C. Oleari, and E. Re, "A general framework for implementing NLO calculations in shower Monte Carlo programs: the POWHEG BOX," *JHEP* **06** (2010) 043, arXiv:1002.2581 [hep-ph].

[182] S. Frixione, P. Nason, and G. Ridolfi, "A Positive-weight next-to-leading-order Monte Carlo for heavy flavour hadroproduction," *JHEP* **09** (2007) 126, arXiv:0707.3088 [hep-ph].

[183] P. Nason, "A New method for combining NLO QCD with shower Monte Carlo algorithms," *JHEP* **11** (2004) 040, arXiv:hep-ph/0409146.

[184] E. Bothmann *et al.*, "Event generation with Sherpa 2.2," *SciPost Phys.* **7** no. 3, (2019) 034, arXiv:1905.09127 [hep-ph].

[185] S. Höche, F. Krauss, S. Schumann, and F. Siegert, "QCD matrix elements and truncated showers," *JHEP* **05** (2009) 053, arXiv:0903.1219 [hep-ph].

[186] S. Höche, F. Krauss, M. Schönherr, and F. Siegert, "QCD matrix elements + parton showers. The NLO case," *JHEP* **04** (2013) 027, arXiv:1207.5030 [hep-ph].

[187] **NNPDF** Collaboration, R. D. Ball *et al.*, "Parton distributions for the LHC run II," *JHEP* **04** (2015) 040, arXiv:1410.8849 [hep-ph].

[188] ATLAS Collaboration, "Example ATLAS tunes of PYTHIA8, PYTHIA6 and POWHEG to an observable sensitive to Z boson transverse momentum." ATL-PHYS-PUB-2013-017, 2013. https://cds.cern.ch/record/1629317.

[189] M. Czakon and A. Mitov, "Top++: A program for the calculation of the top-pair cross-section at hadron colliders," *Comput. Phys. Commun.* **185** (2014) 2930, arXiv:1112.5675 [hep-ph].

[190] M. Cacciari, M. Czakon, M. Mangano, A. Mitov, and P. Nason, "Top-pair production at hadron colliders with next-to-next-to-leading logarithmic soft-gluon resummation," *Phys. Lett. B* **710** (2012) 612–622, arXiv:1111.5869 [hep-ph].

[191] P. Kant, O. M. Kind, T. Kintscher, T. Lohse, T. Martini, S. Mölbitz, P. Rieck, and P. Uwer, "HatHor for single top-quark production: Updated predictions and uncertainty estimates for single top-quark production in hadronic collisions," *Comput. Phys. Commun.* **191** (2015) 74–89, arXiv:1406.4403 [hep-ph].

[192] N. Kidonakis, "Two-loop soft anomalous dimensions for single top quark associated production with a W^- or H^-," *Phys. Rev. D* **82** (2010) 054018, arXiv:1005.4451 [hep-ph].

[193] J. M. Campbell and R. K. Ellis, "$t\bar{t}W^{+-}$ production and decay at NLO," *JHEP* **07** (2012) 052, arXiv:1204.5678 [hep-ph].

[194] A. Lazopoulos, T. McElmurry, K. Melnikov, and F. Petriello, "Next-to-leading order QCD corrections to $t\bar{t}Z$ production at the LHC," *Phys. Lett. B* **666** (2008) 62–65, arXiv:0804.2220 [hep-ph].

[195] R. Gavin, Y. Li, F. Petriello, and S. Quackenbush, "FEWZ 2.0: A code for hadronic Z production at next-to-next-to-leading order," arXiv:1011.3540 [hep-ph].

[196] **LHC Higgs Cross Section Working Group** Collaboration, D. de Florian *et al.*, "Handbook of LHC Higgs Cross Sections: 4. Deciphering the Nature of the Higgs Sector," arXiv:1610.07922 [hep-ph].

[197] ATLAS Collaboration, "Performance of the ATLAS track reconstruction algorithms in dense environments in LHC Run 2," *Eur. Phys. J. C* **77** (2017) 673, arXiv:1704.07983 [hep-ex].

[198] R. Frühwirth, "Application of Kalman filtering to track and vertex fitting," *Nucl. Instrum. Methods Phys. Res., A* **262** no. HEPHY-PUB-503, (Jun, 1987) 444. 19 p. https://cds.cern.ch/record/178627.

[199] T. Cornelissen, M. Elsing, I. Gavrilenko, W. Liebig, E. Moyse, and A. Salzburger, "The new ATLAS track reconstruction (NEWT)," *J. Phys.: Conf. Ser.* **119** (2008) 032014. https://cds.cern.ch/record/1176900.

[200] ATLAS Collaboration, "Vertex Reconstruction Performance of the ATLAS Detector at $\sqrt{s} = 13$ TeV." ATL-PHYS-PUB-2015-026, 2015. https://cds.cern.ch/record/2037717.

[201] ATLAS Collaboration, "Reconstruction of primary vertices at the ATLAS experiment in Run 1 proton–proton collisions at the LHC," *Eur. Phys. J. C* **77** (2017) 332, arXiv:1611.10235 [hep-ex].

[202] ATLAS Collaboration, "Topological cell clustering in the ATLAS calorimeters and its performance in LHC Run 1," *Eur. Phys. J. C* **77** (2017) 490, arXiv:1603.02934 [hep-ex].

[203] ATLAS Collaboration, "Electron and photon performance measurements with the ATLAS detector using the 2015–2017 LHC proton–proton collision data," *JINST* **14** (2019) P12006, arXiv:1908.00005 [hep-ex].

[204] ATLAS Collaboration, "Measurement of the photon identification efficiencies with the ATLAS detector using LHC Run 2 data collected in 2015 and 2016," *Eur. Phys. J. C* **79** (2019) 205, arXiv:1810.05087 [hep-ex].

[205] ATLAS Collaboration, "Electron and photon energy calibration with the ATLAS detector using 2015–2016 LHC proton–proton collision data," *JINST* **14** (2019) P03017, arXiv:1812.03848 [hep-ex].

[206] ATLAS Collaboration, "Electron reconstruction and identification in the ATLAS experiment using the 2015 and 2016 LHC proton–proton collision data at $\sqrt{s} = 13\,\text{TeV}$," *Eur. Phys. J. C* **79** (2019) 639, arXiv:1902.04655 [hep-ex].

[207] ATLAS Collaboration, "Muon reconstruction performance of the ATLAS detector in proton–proton collision data at $\sqrt{s} = 13\,\text{TeV}$," *Eur. Phys. J. C* **76** (2016) 292, arXiv:1603.05598 [hep-ex].

[208] **ATLAS** Collaboration, "Muon reconstruction and identification efficiency in ATLAS using the full Run 2 pp collision data set at $\sqrt{s} = 13$ TeV," arXiv:2012.00578 [hep-ex].

[209] M. Cacciari, G. P. Salam, and G. Soyez, "The anti-k_t jet clustering algorithm," *JHEP* **04** (2008) 063, arXiv:0802.1189 [hep-ph].

[210] M. Cacciari, G. P. Salam, and G. Soyez, “FastJet user manual,” *Eur. Phys. J. C* **72** (2012) 1896, arXiv:1111.6097 [hep-ph].

[211] M. Cacciari, “FastJet: A Code for fast k_t clustering, and more,” in *Deep inelastic scattering. Proceedings, 14th International Workshop, DIS 2006, Tsukuba, Japan, April 20-24, 2006*, pp. 487–490. 2006. arXiv:hep-ph/0607071 [hep-ph]. [,125(2006)].

[212] **ATLAS** Collaboration, G. Aad *et al.*, “Jet energy scale and resolution measured in proton-proton collisions at $\sqrt{s} = 13$ TeV with the ATLAS detector,” arXiv:2007.02645 [hep-ex].

[213] M. Cacciari and G. P. Salam, “Pileup subtraction using jet areas,” *Phys. Lett. B* **659** (2008) 119–126, arXiv:0707.1378 [hep-ph].

[214] ATLAS Collaboration, “Jet energy measurement with the ATLAS detector in proton–proton collisions at $\sqrt{s} = 7$ TeV,” *Eur. Phys. J. C* **73** (2013) 2304, arXiv:1112.6426 [hep-ex].

[215] ATLAS Collaboration, “Determination of jet calibration and energy resolution in proton–proton collisions at $\sqrt{s} = 8$ TeV using the ATLAS detector,” arXiv:1910.04482 [hep-ex].

[216] ATLAS Collaboration, “Performance of pile-up mitigation techniques for jets in pp collisions at $\sqrt{s} = 8$ TeV using the ATLAS detector,” *Eur. Phys. J. C* **76** (2016) 581, arXiv:1510.03823 [hep-ex].

[217] ATLAS Collaboration, “Optimisation and performance studies of the ATLAS b-tagging algorithms for the 2017-18 LHC run.” ATL-PHYS-PUB-2017-013, 2017. https://cds.cern.ch/record/2273281.

[218] ATLAS Collaboration, “ATLAS b-jet identification performance and efficiency measurement with $t\bar{t}$ events in pp collisions at $\sqrt{s} = 13$ TeV,” *Eur. Phys. J. C* **79** (2019) 970, arXiv:1907.05120 [hep-ex].

[219] ATLAS Collaboration, “Measurements of b-jet tagging efficiency with the ATLAS detector using $t\bar{t}$ events at $\sqrt{s} = 13$ TeV,” *JHEP* **08** (2018) 089, arXiv:1805.01845 [hep-ex].

[220] ATLAS Collaboration, “Performance of missing transverse momentum reconstruction with the ATLAS detector using proton–proton collisions at $\sqrt{s} = 13$ TeV,” *Eur. Phys. J. C* **78** (2018) 903, arXiv:1802.08168 [hep-ex].

[221] **ATLAS Collaboration** Collaboration, “$E_{\mathrm{T}}^{\mathrm{miss}}$ performance in the ATLAS detector using 2015-2016 LHC p-p collisions,” Tech. Rep. ATLAS-CONF-2018-023, CERN, Geneva, Jun, 2018. http://cds.cern.ch/record/2625233.

[222] D. Adams *et al.*, “Recommendations of the Physics Objects and Analysis Harmonisation Study Groups 2014,” Tech. Rep. ATL-PHYS-INT-2014-018, CERN, Geneva, Jul, 2014. https://cds.cern.ch/record/1743654.

[223] M. Cacciari, G. P. Salam, and G. Soyez, “The Catchment Area of Jets,” *JHEP* **04** (2008) 005, arXiv:0802.1188 [hep-ph].

[224] **UA1** Collaboration, G. Arnison *et al.*, “Experimental Observation of Isolated Large Transverse Energy Electrons with Associated Missing Energy at $\sqrt{s} = 540$ GeV,” *Phys. Lett. B* **122** (1983) 103–116.

[225] **Aachen-Annecy-Birmingham-CERN-Helsinki-London(QMC)-Paris(CdF)-Riverside-Rome-Rutherford-Saclay(CEN)-Vienna** Collaboration, G. Arnison *et al.*, "Further evidence for charged intermediate vector bosons at the SPS collider," *Phys. Lett. B* **129** no. CERN-EP-83-111, (Jun, 1985) 273–282. 17 p. https://cds.cern.ch/record/163856.

[226] D. R. Tovey, "On measuring the masses of pair-produced semi-invisibly decaying particles at hadron colliders," *JHEP* **04** (2008) 034, `arXiv:0802.2879 [hep-ph]`.

[227] G. Polesello and D. R. Tovey, "Supersymmetric particle mass measurement with the boost-corrected contransverse mass," *JHEP* **03** (2010) 030, `arXiv:0910.0174 [hep-ph]`.

[228] **ATLAS** Collaboration, G. Aad *et al.*, "Performance of the missing transverse momentum triggers for the ATLAS detector during Run-2 data taking," *JHEP* **08** (2020) 080, `arXiv:2005.09554 [hep-ex]`.

[229] **ATLAS** Collaboration, G. Aad *et al.*, "Performance of algorithms that reconstruct missing transverse momentum in $\sqrt{s} = 8$ TeV proton-proton collisions in the ATLAS detector," *Eur. Phys. J. C* **77** no. 4, (2017) 241, `arXiv:1609.09324 [hep-ex]`.

[230] ATLAS Collaboration, "ATLAS data quality operations and performance for 2015–2018 data-taking," *JINST* **15** (2020) P04003, `arXiv:1911.04632 [physics.ins-det]`.

[231] ATLAS Collaboration, "Selection of jets produced in 13 TeV proton–proton collisions with the ATLAS detector." ATLAS-CONF-2015-029, 2015. https://cds.cern.ch/record/2037702.

[232] N. Hartmann, "ahoi." https://gitlab.com/nikoladze/ahoi, 2018.

[233] **ATLAS** Collaboration, "Object-based missing transverse momentum significance in the ATLAS detector," Tech. Rep. ATLAS-CONF-2018-038, CERN, Geneva, Jul, 2018. https://cds.cern.ch/record/2630948.

[234] A. Roodman, "Blind analysis in particle physics," *eConf* **C030908** (2003) TUIT001, `arXiv:physics/0312102`.

[235] ATLAS Collaboration, "A method for the construction of strongly reduced representations of ATLAS experimental uncertainties and the application thereof to the jet energy scale." ATL-PHYS-PUB-2015-014, 2015. https://cds.cern.ch/record/2037436.

[236] J. Bellm *et al.*, "Herwig 7.0/Herwig++ 3.0 release note," *Eur. Phys. J.* **C76** no. 4, (2016) 196, `arXiv:1512.01178 [hep-ph]`.

[237] ATLAS Collaboration, "Simulation of top-quark production for the ATLAS experiment at $\sqrt{s} = 13$ TeV." ATL-PHYS-PUB-2016-004, 2016. https://cds.cern.ch/record/2120417.

[238] S. Frixione, E. Laenen, P. Motylinski, C. White, and B. R. Webber, "Single-top hadroproduction in association with a W boson," *JHEP* **07** (2008) 029, `arXiv:0805.3067 [hep-ph]`.

[239] **ATLAS Collaboration** Collaboration, "SUSY July 2020 Summary Plot Update," Tech. Rep. ATL-PHYS-PUB-2020-020, CERN, Geneva, Jul, 2020. http://cds.cern.ch/record/2725258.

[240] G. Apollinari, I. Béjar Alonso, O. Brüning, M. Lamont, and L. Rossi, *High-Luminosity Large Hadron Collider (HL-LHC): Preliminary Design Report*. CERN Yellow Reports: Monographs. CERN, Geneva, 2015. https://cds.cern.ch/record/2116337.